

CONSTRAINTS ON COSMOLOGICAL PARAMETERS WITH THE BAO MEASUREMENTS FROM DESI (2024)

INTERNSHIP REPORT

BACHELOR'S DEGREE

IN

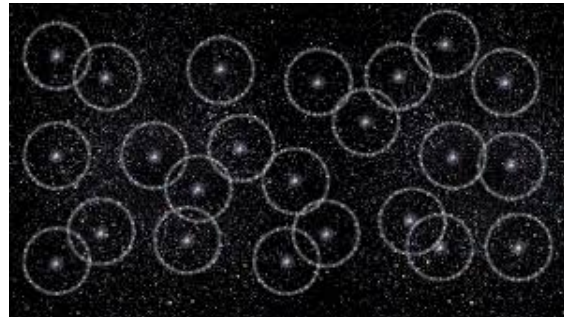
PHYSICS

by

Adrian SZPILFIDEL

Under the guidance of

Alain Blanchard



Institut de Recherche en Astrophysique et en Planétologie (IRAP)

UNIVERSITÉ PAUL SABATIER

Toulouse, France

From July 10th 2024 to August 11th 2024



Acknowledgments

I would like to express my gratitude to Alain Blachard for supervising me during my internship and for giving me the opportunity to explore cosmology.

I also want to thank Brahim Lamine and Isaac Tutusaus from the cosmology team at IRAP for welcoming me into the team. I am grateful for the invitation to the “Cosmology at the Summit” presentation at Pic du Midi.

Lastly, thank you to the team of interns for making me feel welcome.

Abstract

I present the results of my two-month internship at IRAP in cosmology. I worked on the Baryon Acoustic Oscillations (BAO) measurements provided by DESI Collaboration et al. 2024. The main objective of my internship was to demonstrate the acceleration of the expansion and to constrain the cosmological parameters. DESI BAO provides measurements of the transverse comoving distance in seven redshift bins from over 6 million extragalactic objects in the redshift range $0.1 < z < 4.2$. The BAO data are in agreement with the Flat Λ CDM model, with $\Omega_m = 0.289 \pm 0.014$ and $H_0 r_d = (102.4^{+1.3}_{-1.2}) 100 \text{ km s}^{-1}$. Relaxing the ω value, working with the Flat w CDM model, DESI BAO requires $\Omega_m = 0.286 \pm 0.015$; $(102.7^{+3.4}_{-3.1}) 100 \text{ km s}^{-1}$ and $\omega = -1.03 \pm 0.13$. These results are consistent with an accelerated expansion and with the current cosmological model. In the model that probes the dynamics behind dark energy, such as the $\omega_0 \omega_a$ CDM model, the BAO requires $\omega_0 = 1.0^{+1.1}_{-1.0}$ and $\omega_a = -4.0^{+1.9}_{-2.2}$. The BAO does not enable us to determine these parameters properly; it needs to be combined with external sources. The BAO enables us to rule out the power law model for the scale factor, with a minimal reduced $\chi^2 = 5.3$. I also worked on cosmological constraints with the Type 1a Supernovae (SN1a) measurements from the Pantheon+ data release, presented in Brout et al. 2022. This work presents cosmological constraints with 1701 light curves, from $z = 0.001$ to $z = 2.26$. The cosmological constraints show a tension over the Hubble constant H_0 between the two cosmological probes. For Flat Λ CDM I find $\Omega_m = 0.333 \pm 0.018$ and $H_0 = 73.25 \pm 0.24$. In the w CDM model, I find $\Omega_m = 0.306^{+0.061}_{-0.078}$; $H_0 = 73.1 \pm 0.3$ and $\omega = -0.88 \pm 0.15$. For the $\omega_0 \omega_a$ CDM model, I find $\omega_0 = -0.89 \pm 0.10$ and $\omega_a = 0.1^{+0.3}_{-1.6}$. I present a comparison between the results of the two papers, and also test the distance duality relation.

Contents

Abreviations	4
Introduction	5
1 Cosmological background	5
1.1 The Scale Factor	6
1.2 The Metric	6
1.3 General Relativity (GR)	6
1.3.1 Einstein's Equation	6
1.3.2 Friedmann's Equation	7
1.3.3 Acceleration of the Expansion	8
1.4 Measuring the universe	8
1.4.1 Redshift	8
1.4.2 Distances	8
2 Measurements of the Baryon Acoustic Oscillations	10
2.1 Tracers	10
2.2 Measurements of the galaxy distance separations	10
2.3 Two-points correlation function	11
3 Methodology of the constraints on the cosmological parameters	12
3.1 Data	12
3.2 Cosmological model of distances	12
3.3 Optimisation of the parameters	13
4 Results	14
4.1 Flat Λ CDM model	15
4.2 Flat w CDM model	16
4.3 Flat $\omega_0\omega_a$ CDM model	18
4.4 Power law cosmological model	19
5 Cosmological constraint using Type 1a Supernovae (SN1a)	21
5.1 Framework of cosmology	21
5.2 Constraints on the cosmological parameters	22
5.2.1 Results for Flat Λ CDM	22
5.2.2 Results for Flat w CDM	23
5.2.3 Biases in the dataset Pantheon+	23
5.2.4 Constraints for w CDM with DESI and Pantheon+	24
5.2.5 Results for Flat $\omega_0\omega_a$ CDM	26
5.3 Distance duality relation between SN1a and BAO	28
Discussion and conclusion	29
Bibliography	29

Abreviations

- BAO** Baryon Acoustic Oscillations. 2, 3, 5, 10–12, 14, 17–19, 21, 25–29
BGS Bright galaxy survey. 10
- CMB** Cosmological Microwave Background. 5, 14, 16, 17, 21, 25
- DESI** Dark Energy Spectroscopic Instrument. 2, 3, 5, 10–12, 14–16, 24, 25, 27–29
- ELG** Emission line galaxies. 10
- FLRW** Friedmann-Lemaître-Robertson-Walker. 6
- GR** General Relativity. 3, 6
- IRAP** Institut de Recherche en Astrophysique et Planétologie. 1, 2, 29
- LRG** Luminous red galaxies. 10
- QSO** Quasars. 10–12
- SDSS** Sloan Digital Sky Survey. 16
- SN1a** Type 1a Supernovae. 2, 3, 5, 14, 16, 19, 21–23, 25–29

Introduction

The expansion of the universe was discovered by Edwin Hubble (Hubble 1929). In the 1990s, two independent teams of astronomers discovered that this expansion is accelerating (Perlmutter et al. 1999, Riess et al. 1998). These discoveries led to the standard cosmological model (Λ CDM), which describes a spatially flat universe ($\Omega_K = 0$) composed of 5% baryonic matter, 25% dark matter, and 70% dark energy, with smaller contributions from radiation and massive neutrinos. Furthermore, the Planck experiments, which have mapped the anisotropies in the Cosmological Microwave Background (CMB), provide strong constraints on cosmological parameters (Planck Collaboration et al. 2020) and confirm the accuracy of the Λ CDM model. Matter in the universe tends to contract it, while dark energy tends to expand it.

In the early universe, matter was concentrated in a smaller volume and existed as a homogeneous plasma. Slight anisotropies created gravitational attraction among baryonic matter. This attraction was counterbalanced by the interaction between photons and baryons, creating acoustic oscillations known as BAO. This phenomenon ended when photons were emitted during recombination (approximately 380,000 years after the Big Bang). The distribution of baryonic matter was fixed and transferred into galaxy clustering. The maximum distance that the wave could travel in the early universe is the sound horizon, r_d . The BAO feature has been stretched with the expansion of the universe, and now galaxies appear at a co-moving separation of r_d . The value of the sound horizon, provided by early-time physics, is approximately 150 Mpc. The sound horizon r_d is a standard ruler, and can be determined by the CMB (Planck Collaboration et al. 2020). By observing the galaxy distribution in the large-scale structures of the universe at different redshifts, one can visualize the evolution of the BAO feature.

The ground-based telescope Dark Energy Spectroscopic Instrument (DESI) provides BAO measurements. The first detection of the BAO feature took place in 2005 (Eisenstein et al. 2005). Improvements in BAO detection followed. Before DESI, the latest observations had mapped a distance-redshift relation in the range $z < 2.5$. Now, DESI covers 14,200 square degrees in the redshift range $0.1 < z < 4.2$ with a sample size ten times larger than previous surveys. Probing the universe using the BAO feature provides strong constraints on cosmological parameters and enables testing of the Λ CDM model.

The structure of this report is as follows. section 1 summarizes the theoretical cosmology concepts used and presents different cosmological models. section 2 presents the measurements of the BAO feature by DESI. section 3 presents the data used in this work and discusses the methodology to compare the model and the data to optimize the model parameters. section 4 summarizes the results of the statistical inferences in the different cosmological models used to fit the experimental values. Finally, section 5 explores another cosmological probe, Type 1a Supernovae (SN1a), and compares the constraints on parameters to those obtained using the BAO. This section also presents the cosmic distance duality relation between these two cosmological probes.

1 Cosmological background

To write this section, I referred to various books and lectures on cosmology. I used Alain Blanchard's cosmology lectures to gain an initial understanding of the subject. Additionally, I consulted several books for a more in-depth exploration (Dodelson 2003; Mo, Bosch, and White 2010).

1.1 The Scale Factor

Since the speed of light is finite, observing distant objects allows us to look back in time. By examining large structures at certain distances, we see objects as they were when the light was emitted. During the time the light travels to us, the universe expands. This expansion can be described by the scale factor a , which represents the evolution of distances in the universe over time. The present value of the scale factor is set to 1. In the past, a was smaller than 1, and in the future, it will be greater than 1.

$$R(t) = a(t)R_0 \quad (1)$$

Here, $R(t)$ is the distance at a given time t , and R_0 is the distance observed today. Looking back in time ($a < 1$), the physical distances were smaller because the universe was more compact.

1.2 The Metric

The proper length is defined by:

$$dl^2 = g_{ij}dx^i dx^j \quad (2)$$

where g_{ij} is the metric tensor. For instance, in 2D Cartesian coordinates: $g_{ij} = \begin{pmatrix} 1 & 0 \\ 0 & 1 \end{pmatrix}$; $dx^1 = dx$ and $dx^2 = dy$. By adding a time dimension $dx^0 = cdt$, we get:

$$ds^2 = g_{\mu\nu}dx^\mu dx^\nu \quad (3)$$

In an expanding universe, two points in space are always proportional to the scale factor. This is the Friedmann-Lemaître-Robertson-Walker (FLRW) metric:

$$g_{\mu\nu} = \begin{pmatrix} -1 & 0 & 0 & 0 \\ 0 & a^2 & 0 & 0 \\ 0 & 0 & a^2 & 0 \\ 0 & 0 & 0 & a^2 \end{pmatrix} \quad (4)$$

Thus:

$$ds^2 = c^2 dt^2 - dl^2 = c^2 dt^2 - a^2 \left(r^2(d\theta^2 + \sin^2 \theta d\phi^2) + \frac{dr^2}{1 - kr^2} \right) \quad (5)$$

where $k = \{0, -1, 1\}$ is the curvature factor. $k = 0$ in a flat universe, $k = -1$ in a closed universe, and $k = 1$ in an open universe.

1.3 General Relativity (GR)

1.3.1 Einstein's Equation

General relativity, developed by Einstein during the 20th century, aims to describe gravity as a consequence of the curvature of space-time. Einstein's equation of GR relates the curvature of space-time to the components of matter and energy in the universe:

$$G_{\mu\nu} + \Lambda g_{\mu\nu} = R_{\mu\nu} - \frac{1}{2}g_{\mu\nu}R + \Lambda g_{\mu\nu} = \frac{8\pi G}{c^4}T_{\mu\nu} \quad (6)$$

Here $G_{\mu\nu} \equiv R_{\mu\nu} - \frac{1}{2}g_{\mu\nu}R$ is the Einstein tensor; $R_{\mu\nu}$ is the Ricci tensor that contains the metric $g_{\mu\nu}$ and its derivatives; $R \equiv g^{\mu\nu}R_{\mu\nu}$ is the Ricci scalar; G is Newton's constant; c is the speed of light in a vacuum; $T_{\mu\nu}$ is the energy-momentum tensor. The left part of the equation is a function of the metric, while the right part is a function of energy.

1.3.2 Friedmann's Equation

The scale factor evolves with time, and studying its evolution gives indications of the evolution of the universe. The expansion rate, also called the Hubble parameter, quantifies the evolution of the scale factor and is defined as follows:

$$H(t) = \frac{\dot{a}}{a} \quad (7)$$

The present value of $H(t)$ is the Hubble constant H_0 . This constant links the velocities and the distances of nearby galaxies, where the expansion is almost stationary. Sometimes, it is convenient to work with the reduced Hubble constant h :

$$h \equiv \frac{H_0}{100 \text{km} \cdot \text{s}^{-1} \cdot \text{Mpc}^{-1}} \quad (8)$$

The Friedmann equation, which derives from (6), describes the evolution of the Hubble parameter:

$$H^2(t) = \frac{8\pi G}{3c^2} \left(\rho(t) + \frac{\rho_{cr} - \rho_0}{a(t)^2} \right) \quad (9)$$

where $\rho(t)$ is the energy density in the universe and ρ_0 is the present value. $\rho_{cr} \equiv \frac{3c^2 H_0^2}{8\pi G}$ is the critical density today.

Using the value of ρ_{cr} in (9), assuming the universe is flat:

$$H^2(t) = H_0^2 \frac{\rho(t)}{\rho_{cr}} \quad (10)$$

$$\iff H(z) = H_0 \sqrt{\frac{\Omega_{m,0}}{a^3} + \frac{\Omega_{r,0}}{a^4} + \Omega_\Lambda} = H_0 E(z) \quad (11)$$

where $\Omega_{m,0} = \frac{\rho_{m,0}}{\rho_{cr}}$ is the matter density today, and similarly for Ω_r and Ω_Λ .

The evolution of the matter density is scaled to a^{-3} because of the mass conservation law; the density decreases with the volume. The evolution of the radiation density is scaled to a^{-4} because of the Stefan-Boltzmann law. If the total density today is equal to the critical density, the space is flat. Otherwise, there is a density of curvature Ω_k scaled by a^{-2} as described in (9).

1.3.3 Acceleration of the Expansion

Einstein's equation (6), considering an isotropic and homogeneous flat universe, gives the second Friedmann equation:

$$\frac{\ddot{a}}{a} = -\frac{4\pi G}{3} \left(\rho + 3\frac{P}{c^2} \right) \quad (12)$$

As one can see, a positively accelerated universe implies that the terms in the parenthesis are negative. If we consider only matter (including dark matter and baryonic matter) and dark energy, it follows that:

$$\rho = \rho_m + \rho_\Lambda$$

Using the dark energy equation of state:

$$P = \omega \rho_\Lambda \quad (13)$$

It implies:

$$\rho_m + \rho_\Lambda + 3\omega \rho_\Lambda \propto \Omega_m + \Omega_\Lambda + 3\omega \Omega_\Lambda < 0 \quad (14)$$

And it gives a condition between ω and Ω_m to have an accelerated expansion:

$$\omega < -\frac{1}{3(1 - \Omega_m)} \quad (15)$$

1.4 Measuring the universe

1.4.1 Redshift

The wavelength of light is stretched by the expansion of the universe. It creates a shift in the spectra of light. As the wavelength become longer, the color of light tends to the red. It is the redshift and it is defined as follows :

$$z = \frac{\lambda_{obs} - \lambda_{emis}}{\lambda_{emis}} \quad (16)$$

Because the wavelength of the light has been stretched by the expansion since the light was emitted, then $\lambda_{emis} = a\lambda_{obs}$, thus (16) leads to :

$$1 + z = \frac{1}{a} \quad (17)$$

1.4.2 Distances

Comoving distance

If we consider a photon traveling at the speed c observed at $r = 0$. As the geodesic is null ($ds = 0$), equation (5) along the line of sight($\theta = 0, \phi = 0$) gives :

$$\frac{cdt}{a(t)} = \frac{dr}{\sqrt{1 - kr^2}} = d\chi \quad (18)$$

Therefore, one obtains the comoving distance χ :

$$\iff \chi = c \int_{t_0}^t \frac{dt'}{a(t')} = \int_0^{r_s} \frac{dr}{\sqrt{1 - kr^2}} \quad (19)$$

And :

$$\chi = \begin{cases} r & \text{if } k \geq 0 \\ \sin^{-1}(r) & \text{if } k = +1 \\ \sinh^{-1}(r) & \text{if } k = -1 \end{cases} \quad (20)$$

$$\chi = c \int_{t_s}^{t_0} \frac{dt'}{a(t')} \quad (21)$$

Since $H(t) = \frac{da}{dt} \frac{1}{a}$, then $dt = \frac{da}{a(t)H(t)}$

$$\chi = c \int_a^1 \frac{da'}{a'^2 H(a')} \quad (22)$$

And the change of variable $a \rightarrow \frac{1}{1+z}$ gives $da = -\frac{dz}{(1+z)^2}$:

$$\chi = c \int_0^{z_s} \frac{dz}{H(z)} \quad (23)$$

Angular distance

When one is looking at an object with a proper size l at a large distance, the angle of observation is :

$$\theta = \frac{l}{D_A} \quad (24)$$

The comoving size of the object is l/a . So the angle is $\theta = \frac{l/a}{\chi}$. By injecting this form in (35), it gives the angular distance D_A :

$$D_A(z) = a\chi(z) \quad (25)$$

Luminosity distance

The observed flux of an object with a luminosity L at the distance d is :

$$F = \frac{L}{4\pi D_L^2} \quad (26)$$

On a comoving grid the flux is :

$$F = \frac{L(\chi)}{4\pi\chi^2} \quad (27)$$

Let's assume that the luminosity is the energy times the number of photons. The energy that go through a surface at is smaller with the expansion, multiplied by a factor a^2 .

Thus :

$$\begin{aligned} F &= \frac{La^2}{4\pi\chi^2} = \frac{L}{4\pi D_L^2} \\ \iff D_L &= \frac{\chi}{a} \end{aligned} \quad (28)$$

Distance along the line of sight

Considering two points in the space aligned along the line of sight, separated by a distance d . A difference of redshift can be observed between the two objects $\Delta z = |z_1 - z_2|$.

The equation (23) gives the expression of d :

$$d = c \int_{z_1}^{z_2} \frac{dz}{H(z)} \approx \Delta z \frac{c}{H(z)} \quad (29)$$

And :

$$\Delta z = \frac{d}{D_H} \quad (30)$$

Then :

$$D_H(z) = \frac{c}{H(z)} \quad (31)$$

2 Measurements of the Baryon Acoustic Oscillations

2.1 Tracers

DESI covers 6 different types of tracers :

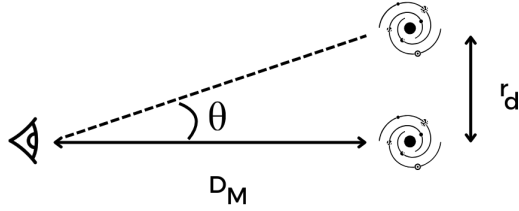
- Low z galaxies of the Bright galaxy survey (BGS) ($0.1 < z < 0.4$)
- Luminous red galaxies(LRG1 & LRG2) ($0.4 < z < 0.6$) & ($0.6 < z < 0.8$)
- Emission line galaxies (ELG) ($1.1 < z < 1.6$)
- Quasars (QSO) ($0.8 < z < 2.1$)
- Lyman- α forest quasars (Ly α) ($1.77 < z < 4.16$)

For each tracers, DESI measures an effective redshift and angle that correspond to the sound horizon r_d at a certain redshift.

2.2 Measurements of the galaxy distance separations

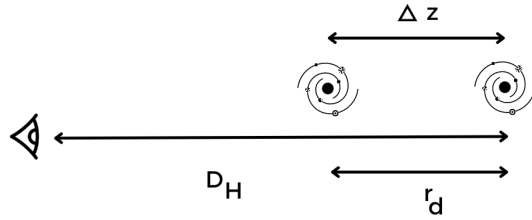
DESI measures **angle separation θ** and **difference of redshift Δz** between pairs of galaxies in each tracer.

When the galaxy are aligned perpendicularly to the line of sight, an angle θ is observed :



$$\theta = \frac{r_d}{D_M}$$

When the galaxy are aligned along the line of sight, an difference of redshift Δz is observed :



$$\Delta z = \frac{r_d}{D_H}$$

Then the angle average distance is given by :

$$D_V(z) = (z D_M(z)^2 D_H(z))^{1/3} \quad (32)$$

For Ly α and QSO, because the signal-to-noise is too low, the data are given in term of D_V/r_d .

2.3 Two-points correlation function

The Dark Energy Spectroscopic Instrument (DESI) measuring galaxiy separation distances over the different tracers presented above. The Baryon Acoustic Oscillations (BAO) feature appears as a peak in the two point correlation function that depends on the separation distance (see Figure 1). The angle corresponding to this peak is measured by DESI and summarized in the Table 1.

The probablity density to find a galaxy in a volum of space is given by :

$$dP = n dV \quad (33)$$

Where n is the volum density of galaxies.

Then, the density probablity to find a galaxy at a certain distance r from a point in the space is :

$$dp = n(1 + \xi(r)) \quad (34)$$

Where $\xi(r)$ is the two points correlation function. The value of $\xi(r)$ decrease like $1/r$ but there is a peak at a certain $r = r_d$ that is the BAO feature.

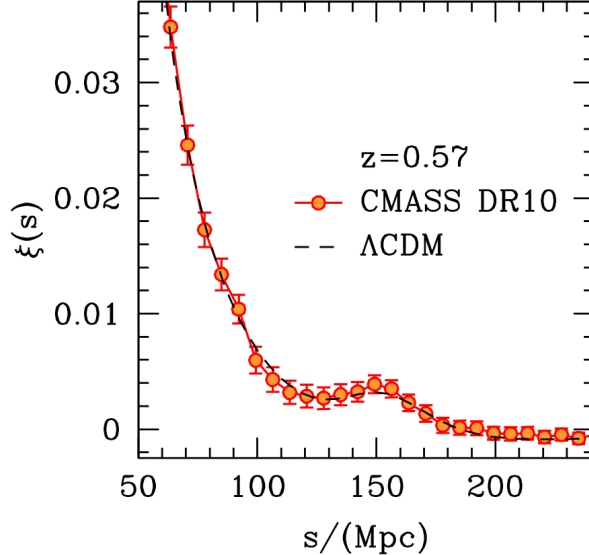


Figure 1: Two-points correlation function from Sánchez et al. 2014

3 Methodology of the constraints on the cosmological parameters

3.1 Data

The data used in this work is the data provided by DESI Collaboration et al. 2024. The data are presented in the Table 1.

tracer	redshift	N_{tracer}	z_{eff}	D_M/r_d	D_H/r_d	r or D_V/r_d	V_{eff} (Gpc 3)
BGS	0.1 – 0.4	300,017	0.295	—	—	7.93 ± 0.15	1.7
LRG1	0.4 – 0.6	506,905	0.510	13.62 ± 0.25	20.98 ± 0.61	-0.445	2.6
LRG2	0.6 – 0.8	771,875	0.706	16.85 ± 0.32	20.08 ± 0.60	-0.420	4.0
LRG3+ELG1	0.8 – 1.1	1,876,164	0.930	21.71 ± 0.28	17.88 ± 0.35	-0.389	6.5
ELG2	1.1 – 1.6	1,415,687	1.317	27.79 ± 0.69	13.82 ± 0.42	-0.444	2.7
QSO	0.8 – 2.1	856,652	1.491	—	—	26.07 ± 0.67	1.5
Lya QSO	1.77 – 4.16	709,565	2.330	39.71 ± 0.94	8.52 ± 0.17	-0.477	—

Table 1: Statistics for the DESI samples used for the DESI DR1 BAO measurements. For each tracer and redshift range one can find the number of objects (N_{tracer}), the effective redshift (z_{eff}) and effective volume (V_{eff}). Note that for each sample we measure either both $D_M/$ and D_H/r_d , which are correlated with a coefficient r , or $D_V/$. Redshift bins are non-overlapping, except for the shot-noise-dominated measurements that use QSO (both as tracers and for Ly α forest).

3.2 Cosmological model of distances

The data of DESI are D_H/r_d and D_M/r_d for each tracers presented in 2.1. The equations (36) and (35) presented in the section 1.4.2 gives the theoretical expression of $D_H(z)$ and $D_M(z)$.

Therefore the model for the three types of measurements are :

$$\frac{D_M}{r_d} = \frac{c}{H_0 r_d} \int_0^z \frac{dz'}{E(z')} \quad (35)$$

$$\frac{D_H}{r_d} = \frac{c}{H_0 r_d E(z)} \quad (36)$$

$$\frac{D_V(z)}{r_d} = \frac{1}{r_d} (z D_M(z)^2 D_H(z))^{1/3} \quad (37)$$

3.3 Optimisation of the parameters

Now I need to compare the experimental values of D_H/r_d , D_M/r_d and D_V/r_d with the values given by the model for each redshift, that depends on the values of the cosmological parameters. To do so, I use the χ^2 test :

$$\chi^2 = \Delta D^t \Sigma^{-1} \Delta D \quad (38)$$

Where ΔD is the vector containing the difference between the data and the model. Σ is the covariance matrix.

Lets define the vector ΔD :

$$\Delta D_i = \begin{pmatrix} (D_M/r_d)_{i,exp} - (D_M/r_d)_{i,model} \\ (D_H/r_d)_{i,exp} - (D_H/r_d)_{i,model} \end{pmatrix} \quad (39)$$

It is the vector that contains the difference between the data and the model, for both D_M/r_d and D_H/r_d . There is a ΔD_i vector for each redshift. Since D_M/r_d and D_H/r_d are correlated the χ^2 can be wrote as it follows :

$$\chi_i^2 = \Delta D_i^t \begin{pmatrix} \sigma_1^2 & r_i \sigma_1 \sigma_2 \\ r_i \sigma_1 \sigma_2 & \sigma_2^2 \end{pmatrix}^{-1} \Delta D_i \quad (40)$$

Where σ_1 is the error on $(D_M/r_d)_{i,exp}$ and σ_2 is the error on $(D_H/r_d)_{i,exp}$. r is the vector containing the correlation factors, and r_i is the correlation factor for between one value of each data.

One needs to add the $\chi_{D_V}^2$ to obtain the total value. Since, there is no correlation between the point at different redshifts this χ^2 can be wrote like :

$$\chi_{D_V}^2 = \sum_{z_i} \left(\frac{D_{V,D} - D_{V,M}}{\sigma(D_{V,D})} \right)^2 \quad (41)$$

Therefore the final χ^2 is :

$$\chi^2 = \sum_i \chi_i^2 + \chi_{D_V}^2 \quad (42)$$

The objective of the statistical inference is to minimize the difference between the data and the model. In order to do this, one has to find the values of the parameters that fit the best the data. Minimizing the χ^2 described by (42), gives the optimised parameters of the model. I used bayesian inference, based on the assumption that the likelihood of the parameter are ruling by a gaussian distribution.

When there is one free parameter, the χ^2 is a 1D-grid and the 68% credible interval is given by $\min(\chi^2) + 1$ and the 95% credible interval is given by $\min(\chi^2) + 4$.

When there is two free parameters, the χ^2 is a 2D-grid and the 68% credible interval is given by $\min(\chi^2) + 2.3$ and the 95% credible interval is given by $\min(\chi^2) + 6.18$. A contour can be plot, representing the area of the 2-parameter-space where the χ^2 is smaller than the limit of the credible intervals.

When there is three free parameters, the χ^2 is a 3D-grid. It is now more convinent to work with the likelihood :

$$L(\chi^2) \propto \exp\left[-\frac{\chi^2}{2}\right] \quad (43)$$

In order to obtain the contour plots of the parameters by pairs, one has to marginalize over the third parameter, to reduce the 3D-grid on a 2D-grid. To determine the credible intervals, one has to sum the density probability until the sum is equal to 0.68 or 0.95 following the interval wanted. What I did is that I flatted the 2D array into a 1D array and the I sorted it to sum the values from the higher to the smaller until the sum is equal to 0.68 or 0.95. To plot the likelihood of one parameter, one has to marginalize a second time over the second parameter.

4 Results

The Table 2 summaries all the results from my work.

model/dataset	H_0 [km s $^{-1}$ Mpc $^{-1}$]	Ω_m	ω or ω_0	ω_a	α
FlatΛCDM					
DESI BAO & r_d from CMB	$69.6_{-0.8}^{+0.9}$	0.289 ± 0.014	—	—	—
Pantheon+ SN1a	73.25 ± 0.24	0.333 ± 0.018	—	—	—
FlatwCDM					
DESI BAO & r_d from CMB	$69.8_{-2.1}^{+2.3}$	0.286 ± 0.015	-1.03 ± 0.13	—	—
Pantheon+ SN1a	73.1 ± 0.3	$0.306_{-0.078}^{+0.061}$	-0.88 ± 0.15	—	—
BAO & SN1a & SH0ES	74.0 ± 0.2	$0.239_{-0.011}^{+0.006}$	-0.98 ± -0.04	—	—
Flat$\omega_0\omega_a$CDM					
DESI BAO & r_d from CMB	55.31 ± 0.05	$0.478_{-0.089}^{+0.111}$	$1.0_{-1.0}^{+1.1}$	$-4.0_{-2.2}^{+1.9}$	—
Pantheon+ SN1a	71.86 ± 0.43	$0.525_{-0.075}^{+0.050}$	$-0.69_{-0.10}^{+0.51}$	$-3.18_{-3.55}^{+2.18}$	—
Pantheon+ SN1a & SH0ES Cepheids	73.0 ± 0.4	$0.419_{-0.109}^{+0.067}$	-0.89 ± 0.10	$0.1_{-1.6}^{+0.3}$	—
DESI & Panthon+	—	—	-0.69 ± 0.10	-0.73 ± 0.27	—
DESI & Pantheon+ & SH0ES	—	—	-0.89 ± 0.10	$-0.18_{-0.55}^{+0.27}$	—
Power law					
DESI BAO & r_d from CMB	60.1 ± 0.6	—	—	—	0.91 ± 0.01

Table 2: Summary of the results of the constraints on cosmological parameters using BAO data from DESI, r_d from CMB and the SN1a data from Pantheon+ with calibrators from SH0ES.

4.1 Flat Λ CDM model

The flat universe model implies :

$$\Omega_K = 0 = 1 - \Omega_m - \Omega_\Lambda - \Omega_R \quad (44)$$

Ω_R can be neglected at low redshift. The energy density of matter is $\Omega_m = \Omega_{m,0}(1+z)^3$ and the Hubble parameter is :

$$H(z) = H_0 E(z) = H_0 \sqrt{\Omega_{m,0}(1+z)^3 + \Omega_\Lambda} \quad (45)$$

Here the energy density of dark energy is $\Omega_\Lambda = 1 - \Omega_m$

This expression of the Hubble rate (45) is injected in relations (35), (36) and (37) and there are two free parameters Ω_m and $H_0 r_d$.

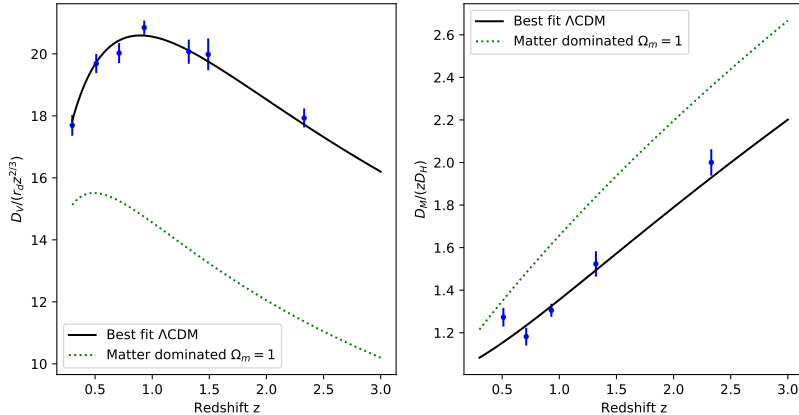


Figure 2: Hubble diagram of the DESI data, the Λ CDM best fit for Ω_m value (black line) and the matter dominated universe model (green dotted line). The left plot is scaled with a factor $z^{-2/3}$ and the right plot with a factor z^{-1} for visualisation purpose.

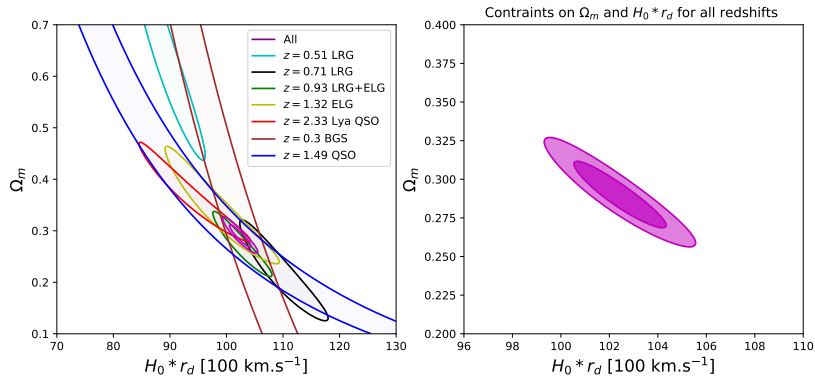


Figure 3: Constraints on Ω_m and $H_0 r_d$ for Λ CDM model. The left plot represents the constraint for each redshift that corresponds to a tracer. The right plot represents the constraints with all the tracers combined. The dark magenta is the 1σ contour and the magenta is the 2σ contour.

One can emphasize that in the Figure 3, the tracers that have only D_V/r_d data are represented by a strive, there is a degenerescence between $H_0 r_d$ and Ω_m while for the tracers that have D_M/r_d and D_H/r_d data, the constraint gives an ellipse.

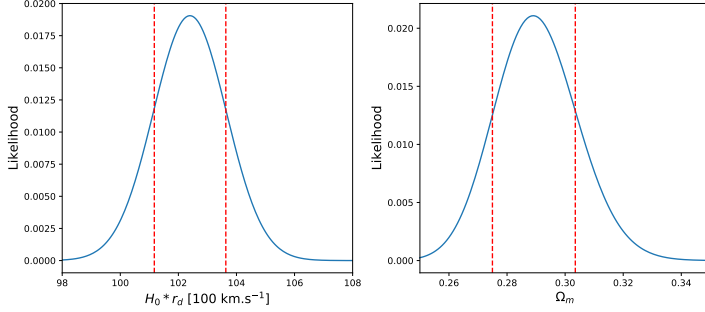


Figure 4: Likelihoods for Ω_m and $H_0 r_d$

$$\boxed{\Omega_m = 0.289 \pm 0.014 \quad | \quad H_0 r_d = (102.4^{+1.3}_{-1.2}) 100 \text{ km s}^{-1} \quad | \quad \chi^2_r = 1.36}$$

Table 3: Results

With the value of r_d from the CMB ($r_d = (147.09 \pm 0.26)$ Mpc), one can deduce the H_0 value :

$$H_0 = (69.62^{+0.89}_{-0.83}) \text{ km s}^{-1} \text{ Mpc}^{-1}$$

Where the uncertainty on H_0 is $u(H_0) = H_0 \sqrt{\left(\frac{u(H_0 r_d)}{H_0 r_d}\right)^2 + \left(\frac{u(r_d)}{r_d}\right)^2}$

Even though these results are slightly shifted from those from DESI in agreement with Collaboration et al. 2024 values for $\Omega_m = 0.295 \pm 0.015$ and $h r_d = (101.8 \pm 1.3)$ Mpc. And furthermore, these values are in agreement with the previous dark energy survey from SDSS Alam et al. 2021.

It means that the universe is composed by 28.9% of matter, which includes baryonic and non-baryonic matter as well. We are today dominated by dark energy $\Omega_\Lambda = 1 - \Omega_m = 0.711 \pm 0.014$.

The value of the Hubble constant is different from the value measured with low z probes such as Type 1a Supernovae (SN1a) where $H_0 \approx 73 \text{ km s}^{-1} \text{ Mpc}^{-1}$ presented in the section 5. This tension is known as the Hubble tension and there is still no consensus on the true value of H_0 .

4.2 FlatwCDM model

The universe is still flat ($\Omega_K = 0$). It describes the dark energy as a fluid, with a state equation $P = \omega \rho_\Lambda$. The energy density of dark energy is given by :

$$\Omega_\Lambda = \Omega_{\Lambda,0}(1+z)^{3(1+\omega)} \tag{46}$$

Thus :

$$H(z) = H_0 \sqrt{\Omega_{m,0}(1+z)^3 + \Omega_{\Lambda,0}(1+z)^{3(1+\omega)}} \tag{47}$$

This expression of the Hubble rate (47) is injected in relations (35), (36) and (37) and there are three free parameters Ω_m , $H_0 r_d$ and ω .

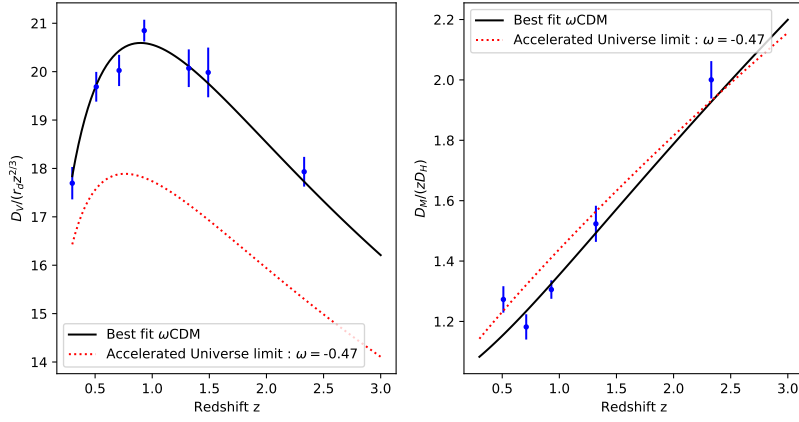


Figure 5: Hubble diagramm of the BAO measurements, scaled with a factor z for visualize purpose. The black line is the fit with the value of ω optimised. The limit of an accelerated expansion (red dotted line) and the matter dominated model (green dotted line) are also represented

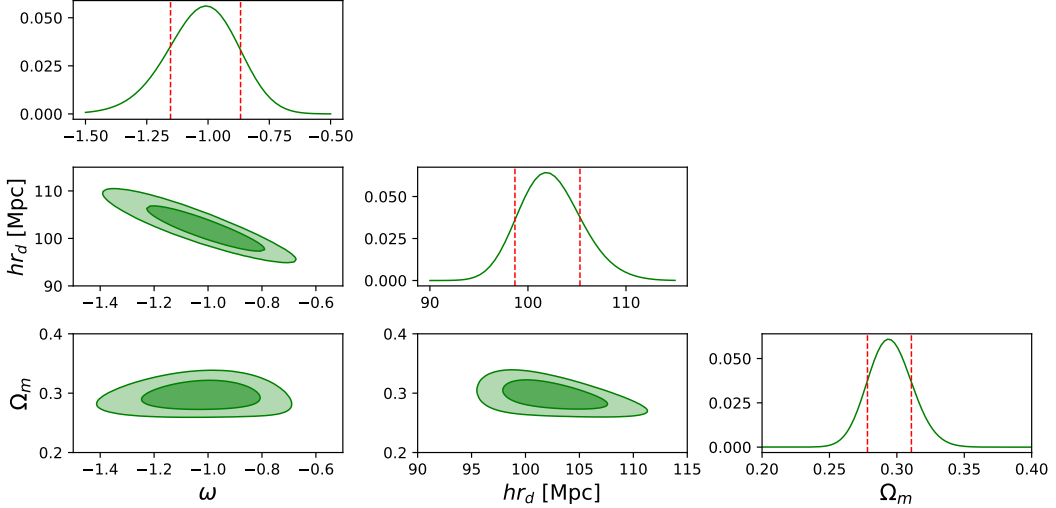


Figure 6: Constraint on all the parameters

$\omega = -1.03 \pm 0.13$	$H_0 r_d = (102.7_{-3.1}^{+3.4}) 100 \text{ km s}^{-1}$	$\Omega_m = 0.286 \pm 0.015$	$\chi^2 = 15.34$
---------------------------	---	------------------------------	------------------

Table 4: Results

With the $H_0 r_d$ value, one can deduce the H_0 value using r_d from CMB :

$$H_0 = (69.8_{-2.1}^{+2.3}) \text{ km s}^{-1} \text{ Mpc}^{-1}$$

$$\text{Where } u(H_0) = H_0 \sqrt{\left(\frac{u(H_0 r_d)}{H_0 r_d}\right)^2 + \left(\frac{u(r_d)}{r_d}\right)^2}$$

Those results are perfectly consistent with DESI Collaboration et al. 2024 : $\Omega_m = 0.293 \pm 0.015$ and $\omega = -0.99_{-0.13}^{+0.15}$.

Now if we look closer to the plot of Ω_m and ω , it gives information about the acceleration of the universe. This acceleration is ruled by the Friedmann equation (12), where the limit of a positive acceleration is given by (15). This limite is computed on the Figure 7. We can affirm that the constraints on the BAO shows that the expansion is accelerated. The 2σ contour is far from the limit computed in dotted line ($\approx 4\sigma$).

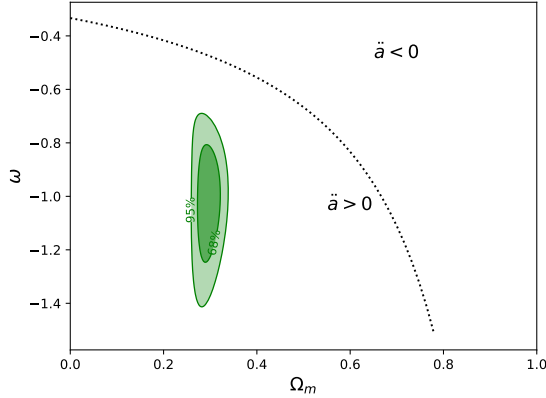


Figure 7: Contour marginalised over $H_0 r_d$. The black dotted line represents the accelerated universe limit. The dark green contour is the 1σ contour while the green is the 2σ .

4.3 Flat $\omega_0\omega_a$ CDM model

This model describe the dark energy not like a constant but as a variable. The $\omega(z)$ state equation parameter of dark energy evolves with time. The expression of ω used in the Hubble parameter $H(z)$ is the following :

$$\omega(z) = \omega_0 + \omega_a(1 - \frac{1}{1+z}) \quad (48)$$

If $\omega_0 = -1$ and $\omega_a = 0$, the model is the Λ CDM model. The constraints of this part is made over 4 free parameters which are : $H_0 r_d$, Ω_m , ω_0 , ω_a .

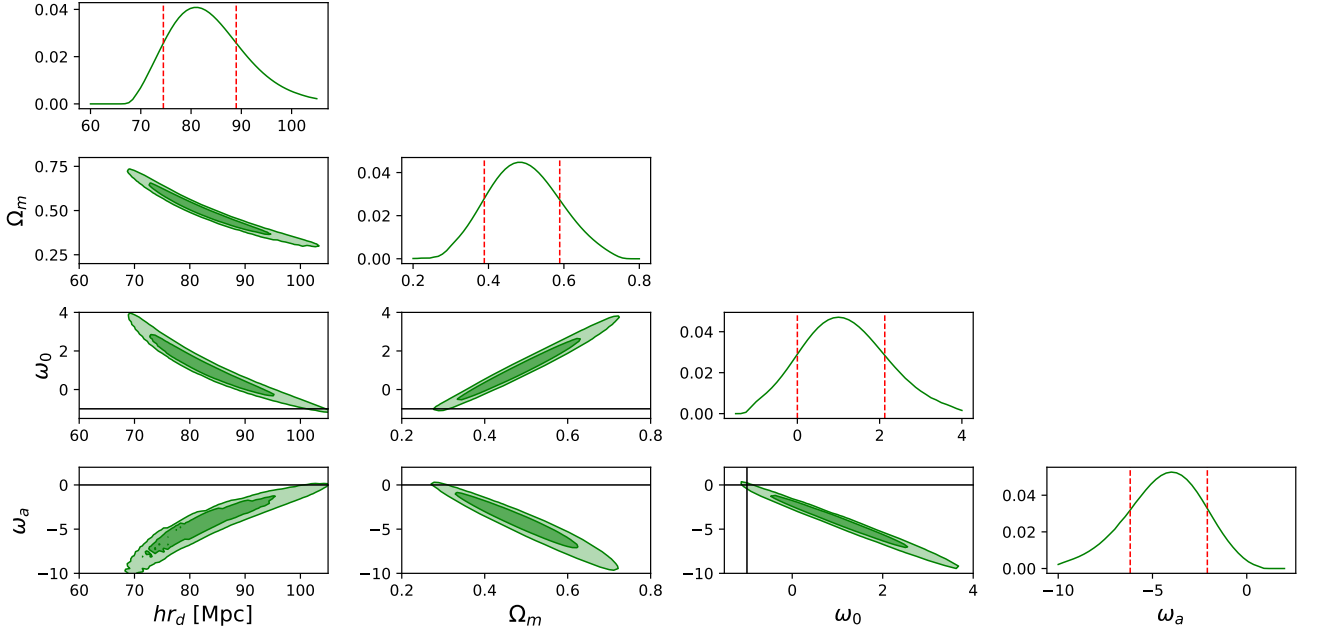


Figure 8: Profile likelihoods for the 4 free parameters for $\omega_0\omega_a$ CDM model. The black lines represents the fiducial value for Λ CDM for ω_0 and ω_a

hr_d [Mpc]	Ω_m	ω_0	ω_a	χ^2_r
$81.4^{+7.6}_{-6.9}$	$0.478^{+0.111}_{-0.089}$	$1.0^{+1.1}_{-1.0}$	$-4.0^{+1.9}_{-2.2}$	1.15

Table 5: Results

By adding a parameter, the constraints became larger. The BAO doesn't show results in contradiction with Λ CDM model. We can see in Figure 8 that the standard value of ω_0 and ω_a are contained in the contours. These results are not fully consistent with DESI Collaboration et al. 2024 because of the priors they used. They cut priors at 1 and 2 for ω_0 and ω_a respectively. This cut has an influence on the final result. They obtained $\Omega_m = 0.344^{+0.047}_{-0.026}$, $\omega_0 = -0.55^{+0.39}_{-0.21}$ and $\omega_a < -1.32$. But their contours are very similar to mine.

In the section subsubsection 5.2.5, the constraint for $\omega_0\omega_a$ CDM is realised by combining the BAO data with the SN1a data, only for the ω_0 and ω_a parameters.

4.4 Power law cosmological model

The objective of a power law model is to give an analytical expression of the scale factor $a(t)$ as a function of time. There are several works on this subject, see Dolgov, Halenka, and Tkachev 2014 and Melia 2024.

For instance, at early time, the universe was dominated by matter, if we assume $\Omega_m = 1$, the Hubble parameter can be written as :

$$\frac{\dot{a}}{a} = H(a) = H_0 a^{-3/2} \quad (49)$$

$$\begin{aligned}
\frac{da}{dt} a^{1/2} &= H_0 \\
\iff \int da a^{1/2} &= H_0 \int dt \\
a^{2/3} &= \frac{3}{2} H_0 t \\
a(t) &= \left(\frac{3}{2} H_0 \right)^{2/3} t^{2/3} = \left(\frac{t}{t_0} \right)^{2/3}
\end{aligned} \tag{50}$$

In the power law cosmological model, the aim is to fit the cosmic expansion with :

$$a(t) = \left(\frac{t}{t_0} \right)^\alpha \tag{51}$$

Calculating the Hubble parameter given by (7) :

$$H(t) = \frac{\alpha}{t} \tag{52}$$

Injecting the expression of $t = t_0 a^{1/\alpha} = \frac{t_0}{(1+z)^{1/\alpha}}$ deduced from (51), the Hubble parameter is :

$$\begin{aligned}
H(z) &= \frac{\alpha}{t_0} (1+z)^{1/\alpha} \\
\iff H(z) &= H_0 (1+z)^{1/\alpha}
\end{aligned} \tag{53}$$

The free parameter are $H_0 r_d$ and α .

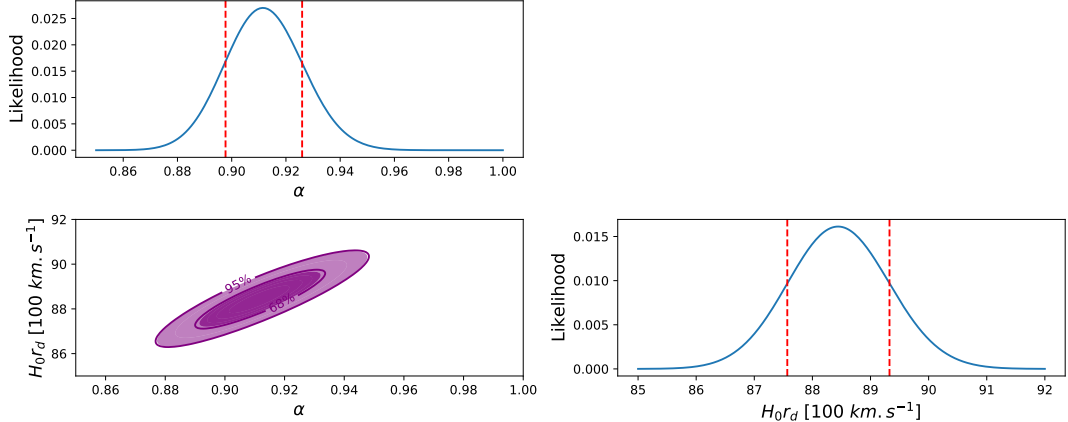


Figure 9: Contours obtained with the constraint on α and $H_0 r_d$

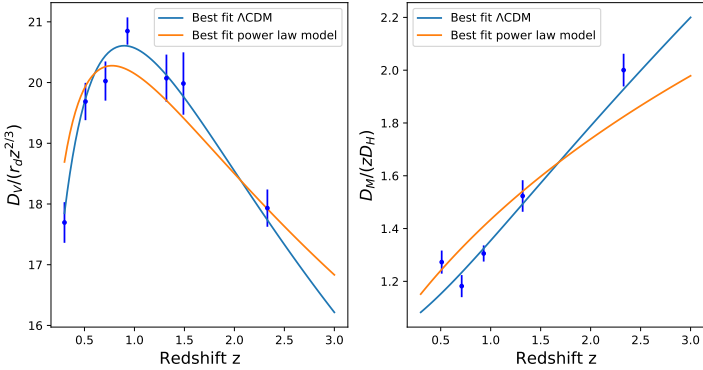


Figure 10: Hubble diagramm with the comparison of the Λ CDM fit and the power law fit

$$\boxed{\alpha = 0.91 \pm 0.01 \quad H_0 r_d = (88.4 \pm 0.9) 100 \text{ km s}^{-1} \quad \chi_r^2 = 5, 3}$$

Table 6: Results

With the $H_0 r_d$ value, one can deduce the H_0 value using r_d from CMB :

$$H_0 = (60.1 \pm 0.6) \text{ km s}^{-1} \text{ Mpc}^{-1}$$

$$\text{Where } u(H_0) = H_0 \sqrt{\left(\frac{u(H_0 r_d)}{H_0 r_d}\right)^2 + \left(\frac{u(r_d)}{r_d}\right)^2}$$

The value of $\chi^2 = 53$ is too high for 12 degree of freedom and 2 free parameters. Consequently, the power law model doesn't provide a robust fit regarding the BAO data. This is in contradiction with the conclusion of recent work, see Melia 2024. Previous work had already disfavored the power law model, see Shafer 2015 and Tutzus et al. 2016.

5 Cosmological constraint using Type 1a Supernovae (SN1a)

5.1 Framework of cosmology

The Type 1a Supernovae are considered as standard candles. As their intrinsic luminosity is well known and is always shining in the same way, by measuring the absolute magnitude received, it is possible to know the luminosity distance. By measuring the redshift and the distance, it is possible to know about the universe expansion. Brout et al. 2022 present a cosmological constraints from the Pantheon+ analysis, these are the data that I will use in this part. In their work they use 1550 SN1a data combined with 151 cepheid host distances presented by the SH0ES team (see Riess et al. 2022).

The distance modulus μ is measured by calibrating on the Cepheids. The model used to fit the values is the following :

$$\mu_{model} = 5 \log(d_L(z)/10\text{pc}) \tag{54}$$

Where D_L is the luminosity distance described by the relation (28).

5.2 Constraints on the cosmological parameters

5.2.1 Results for Flat Λ CDM

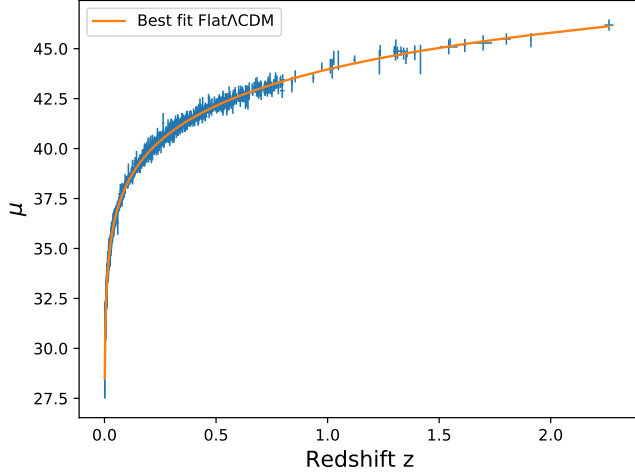


Figure 11: Hubble diagram pour the SN1a distance moduli measurements from Pantheon+. The data are fitted with H_0 and Ω_m as free parameters.

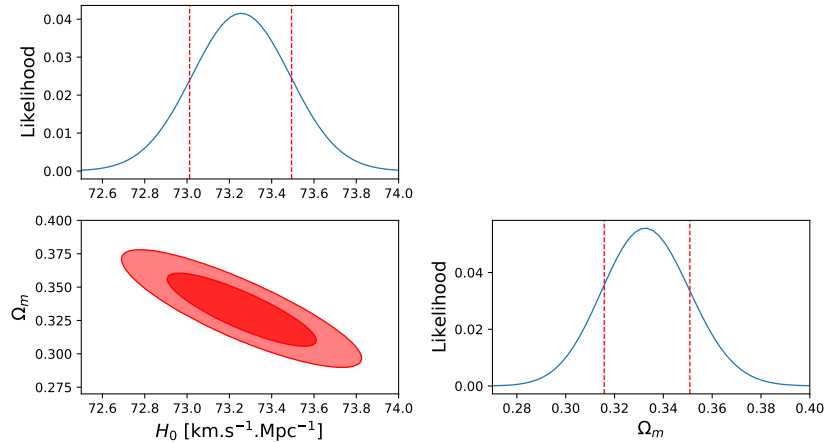


Figure 12: Constraint on 2 free parameters for Λ CDM model. The dark red contour is 1σ and the red is 2σ contour.

$H_0 = (73.25 \pm 0.24) \text{ km s}^{-1} \text{ Mpc}^{-1}$	$\Omega_m = 0.333 \pm 0.018$	$\chi^2_r = 0.90$
---	------------------------------	-------------------

Table 7: Results

The strength of the SN1a is to provide a direct measurement of the Hubble constant. My result on Ω_m is very consistent with the result presented in Brout et al. 2022 where $\Omega_m = 0.334 \pm 0.018$. However, my result for H_0 differs slightly from them where $H_0 = 73.6 \pm 1.1$. My errorbar is lower as well, I don't really understand how they estimated the uncertainty on H_0 .

5.2.2 Results for Flat w CDM

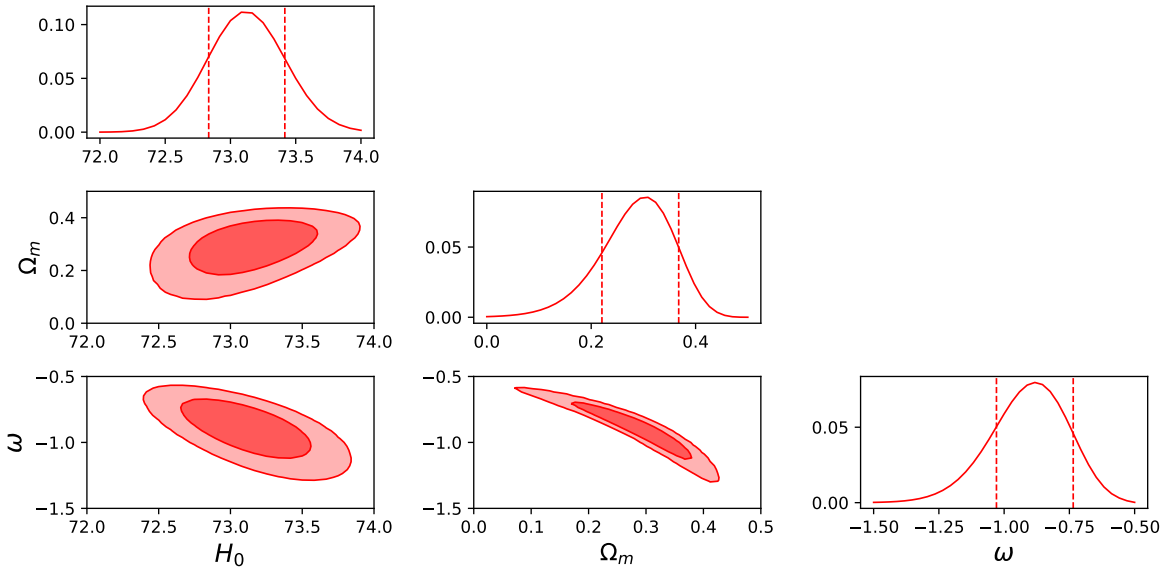


Figure 13: Constraints on 3 free parameters with the SN1a. The dark red are the 1σ contours and the red are the 2σ contours.

$H_0 = (73.1 \pm 0.3) \text{ km s}^{-1} \text{ Mpc}^{-1}$	$\Omega_m = 0.306^{+0.061}_{-0.078}$	$\omega = -0.88 \pm 0.15$	$\chi^2_r = 0.90$
---	--------------------------------------	---------------------------	-------------------

Table 8: Results using Pantheon+ & SH0ES

For the w CDM, Brout et al. 2022 finds $H_0 = 73.5 \pm 1.1$, $\Omega_m = 0.309^{+0.063}_{-0.069}$ and $\omega = -0.90 \pm 0.14$. My results are in agreement with these ones, but for the Hubble constant my 68% credible interval gives thinner errors.

5.2.3 Bias in the dataset Pantheon+

The distance for the low redshift supernovae are calibrated on SH0ES cepheids. This calibration uses a different expression than μ_{model} given by (54). The distance value from SH0ES is more precise than the luminosity distance. Using or not this calibration gives significant difference in the constraint on cosmological parameters (see e.g Figure 14, and Figure 15). The peculiar velocities of nearby galaxies bias the distance moduli value. Cutting the data at $z < 0.01$ or $z < 0.02$ gives also different results for the parameters. This bias has to be considered in the constraint on cosmological parameters.

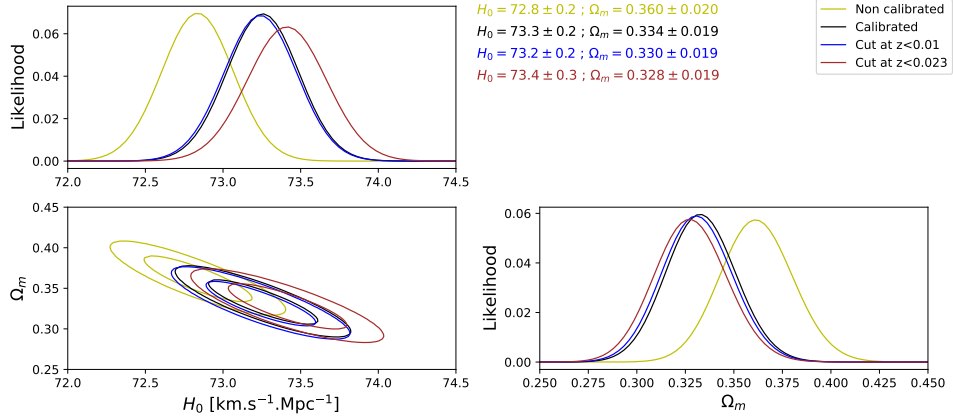


Figure 14: Shift on the constraint for Λ CDM

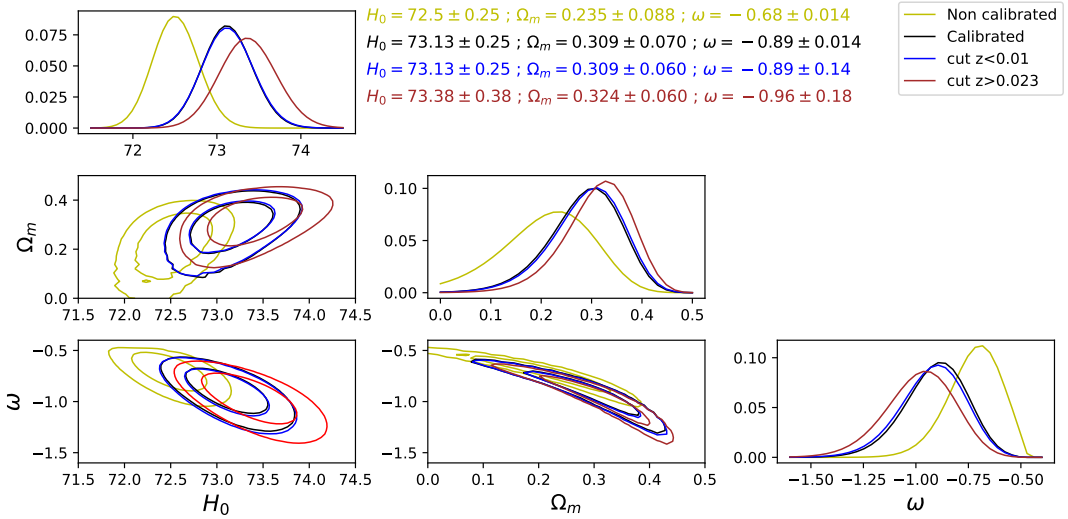


Figure 15: Shift on the constraint for w CDM

Considering the results presented in Brout et al. 2022, it seems that the data used are the one calibrated with Sh0es (represented in black in Figure 14 and Figure 15). The effect of cutting the data at a given redshift is the same whether you use the calibrated data or the non-calibrated. However, this effect is getting smaller when z rises because the influence of the peculiar velocity become less and less significant. One can see this by looking at the Figure 4 of Brout et al. 2022.

5.2.4 Constraints for w CDM with DESI and Pantheon+

It is interesting to combine the data from DESI and Pantheon+ and constraint the parameter to obtain more precise values.

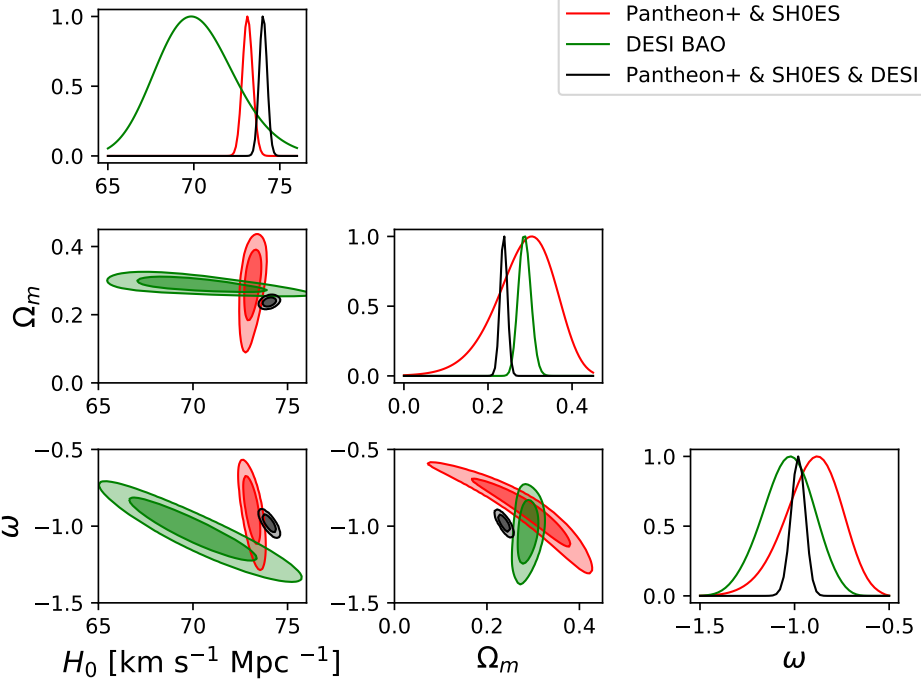


Figure 16: Contours for w CDM model with SN1a data combined with SH0ES (red), BAO + r_d from CMB (green) and both (black).

$H_0 [\text{km s}^{-1} \text{ Mpc}^{-1}]$	Ω_m	ω_0
74.0 ± 0.2	$0.239^{+0.006}_{-0.011}$	-0.98 ± -0.04

Table 9: Results for Pantheon+ and DESI combined

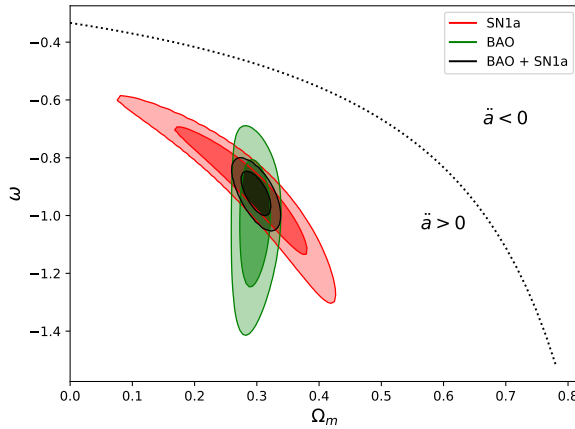


Figure 17: Comparison of SN1a data from Pantheon+ and BAO from DESI on the constraint for w CDM model, marginalised over respectively H_0 and $H_0 r_d$. The black dotted line represents the accelerated universe limit.

We can see in Figure 17 that Pantheon+ and DESI data give a strong evidence of an expansion accelerated of the universe. The black contour is not the same as the one in Figure 16

because here the two χ^2 grids for SN1a and BAO are combined after been marginalised on H_0 .

5.2.5 Results for Flat $\omega_0\omega_a$ CDM

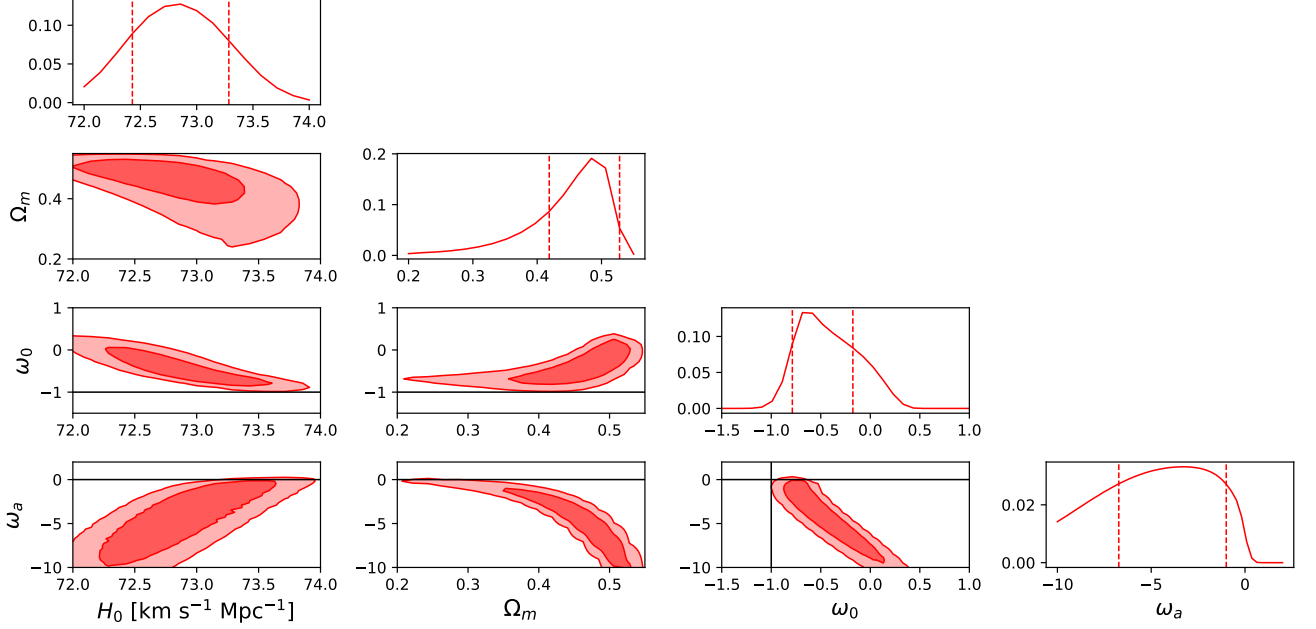


Figure 18: Contours of the constraints for Flat $\omega_0\omega_a$ CDM using SN1a from Pantheon+ only, without using SH0ES calibration on cepheids.

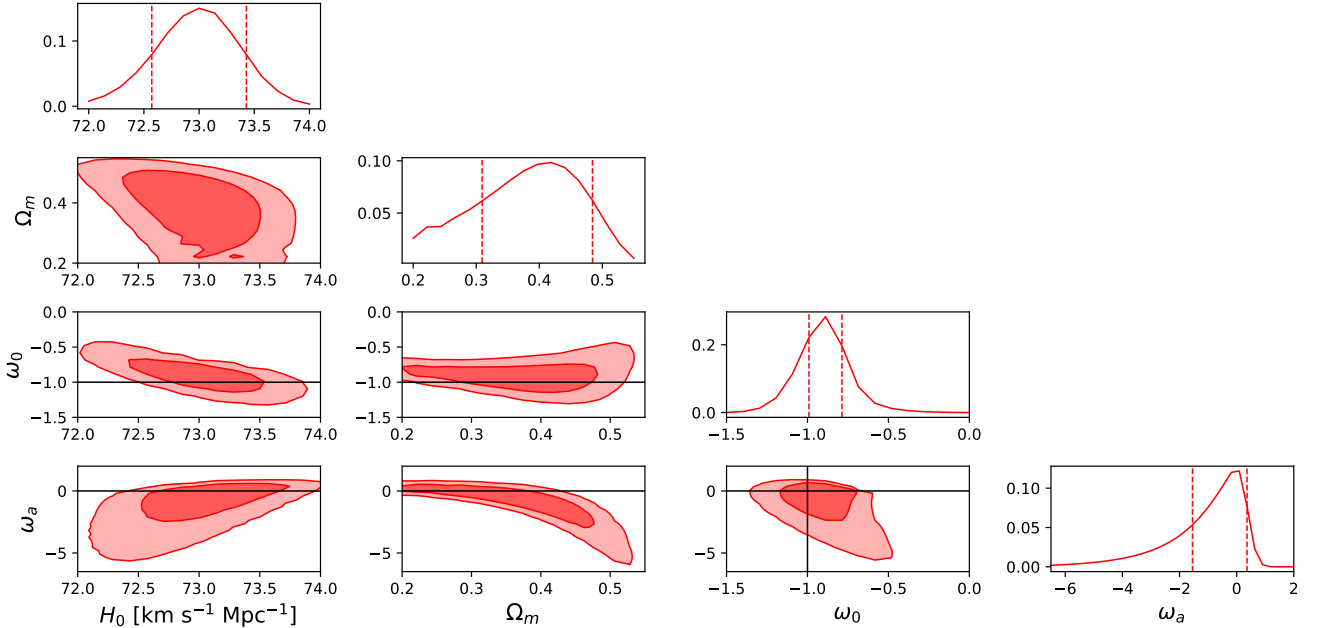


Figure 19: Contours of the constraints for Flat $\omega_0\omega_a$ CDM using SN1a and SH0ES calibration on cepheids.

	H_0 [km s $^{-1}$ Mpc $^{-1}$]	Ω_m	ω_0	ω_a	χ^2_r
Pantheon+	71.86 ± 0.43	$0.525^{+0.050}_{-0.075}$	$-0.69^{+0.51}_{-0.10}$	$-3.18^{+2.18}_{-3.55}$	1.03
Pantheon+ & SH0ES	73.0 ± 0.4	$0.419^{+0.067}_{-0.109}$	-0.89 ± 0.10	$0.1^{+0.3}_{-1.6}$	0.90

Table 10: Results

As we saw on the constraints using BAO in Figure 8, the SN1a only doesn't provide a strong constraint on the parameters for the Flat $\omega_0\omega_a$ CDM model (see Figure 18 and Figure 19). The standard value of Λ CDM are still in the contours in Figure 19. The results of Figure 18 are biased by peculiar velocities at low redshift because I didn't use the calibration, as explain in subsubsection 5.2.3. The results on the parameters (Table 10) are not optimal because the number of point for each parameter grid is not high enough. The reason is that the computing is very long.

Combining with DESI BAO :

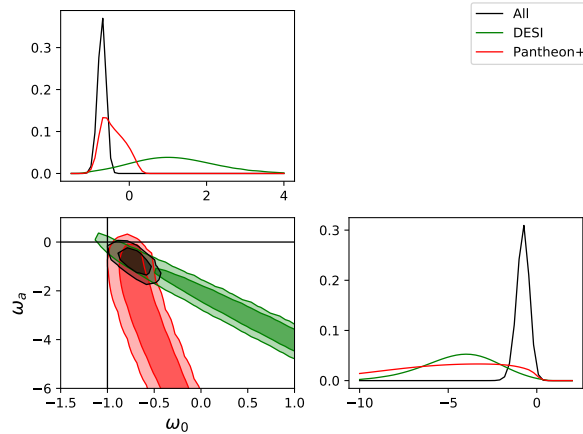


Figure 20: Contour plot of ω_a with respect to ω_0 for BAO (green), SN1a (red) and both combined (black).

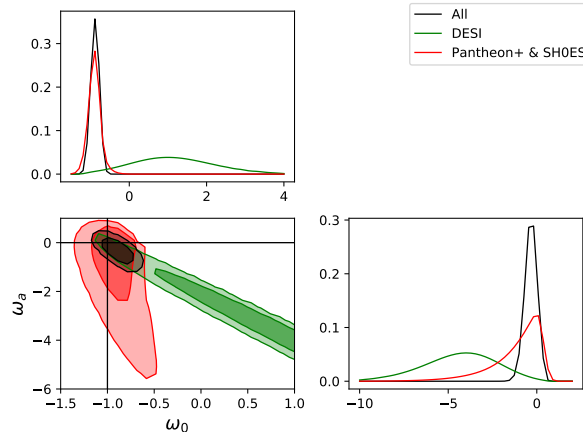


Figure 21: Contour plot of ω_a with respect to ω_0 for BAO (green), SN1a+SH0ES cepheids (red) and both combined (black).

	ω_0	ω_a
Pantheon+ & DESI	-0.69 ± 0.10	-0.73 ± 0.27
Pantheon+ & SH0ES & DESI	-0.89 ± 0.10	$-0.18^{+0.27}_{-0.55}$

Table 11: Results

As one can see in Figure 21, the contour is in agreement with Λ CDM, represented by the black lines intersection. The low redshift data can bias the results, this is illustrated by Figure 20.

5.3 Distance duality relation between SN1a and BAO

It is interesting to test whether the distance measurements between the two probes correspond or not. If they do not, it would imply that there is new physics to develop or there are systematic errors that were not well controlled. There is a very recent work presented by Wang et al. 2024 on this subject.

Since there is a tension on the Hubble constant value, which is $H_{0,\text{SN}} \approx 74 \text{ km s}^{-1} \text{ Mpc}^{-1}$, while the value measured in the early universe is $H_{0,\text{CMB}} \approx 67 \text{ km s}^{-1} \text{ Mpc}^{-1}$. To manage this Hubble tension, I did not fix a value of H_0 and left it as a free parameter.

In order to test the distance duality relation, I took the Ω_m best value from the constraint using only SN1a data. Then I converted the luminosity distance into an angular distance by dividing it by the scale factor a . Since DESI BAO measurements are expressed in the form of distance over r_d , I had to divide the angular distance of SN1a by r_d and then constrain the $H_0 r_d$ with the BAO values.

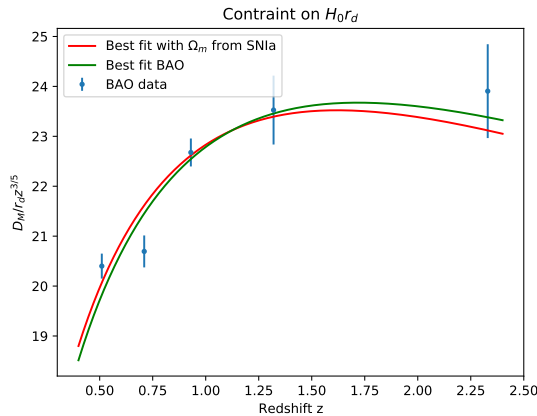


Figure 22: Constraint on $H_0 r_d$ with SN1a and BAO

SN1a	$H_0 r_d = (99.00^{+0.82}_{-0.80}) 100 \text{ km s}^{-1}$	$\chi^2 = 8.33$
BAO	$H_0 r_d = (101.9^{+3.3}_{-3.0}) 100 \text{ km s}^{-1}$	$\chi^2 = 7.15$

Table 12: Results

These results confirm the cosmic duality distance relation between the SN1a and the BAO.

Discussion and conclusion

In this work, I have summarized all my activities during my internship at Institut de Recherche en Astrophysique et Planétologie (IRAP). I delved into the field of cosmology by studying the expansion of the universe using Baryon Acoustic Oscillations (BAO) and Type 1a Supernovae (SN1a). I replicated the research conducted by Collaboration et al. 2024 and Brout et al. 2022, and my results on cosmological constraints are consistent with theirs. I analyzed the data provided by Dark Energy Spectroscopic Instrument (DESI) and Pantheon+ using various cosmological models such as Λ CDM, w CDM, $\omega_0\omega_a$ CDM, and the power law model. I focused on flat universe models ($\Omega_k = 0$), but these data also allow for the curvature parameter to be varied. However, the distance must be considered in its full expression. These results reveal a tension in the Hubble constant between these two datasets. I found that the SN1a data are sensitive to the calibration on Cepheids with Sh0es, introducing a shift in the cosmological constraints. The magnitude of this shift has an influence on the results in Flat $\omega_0\omega_a$ CDM model. The constraint on ω_0 and ω_a using Pantheon+, SH0ES and DESI doesn't show any dynamic behind dark energy.

References

- [1] Shadab Alam et al. “Completed SDSS-IV extended Baryon Oscillation Spectroscopic Survey: Cosmological implications from two decades of spectroscopic surveys at the Apache Point Observatory”. In: 103.8, 083533 (Apr. 2021), p. 083533. DOI: [10.1103/PhysRevD.103.083533](https://doi.org/10.1103/PhysRevD.103.083533). arXiv: [2007.08991 \[astro-ph.CO\]](https://arxiv.org/abs/2007.08991).
- [2] Dillon Brout et al. “The Pantheon+ Analysis: Cosmological Constraints”. In: *The Astrophysical Journal* 938.2 (Oct. 2022), p. 110. DOI: [10.3847/1538-4357/ac8e04](https://doi.org/10.3847/1538-4357/ac8e04). URL: <https://dx.doi.org/10.3847/1538-4357/ac8e04>.
- [3] DESI Collaboration et al. *DESI 2024 VI: Cosmological Constraints from the Measurements of Baryon Acoustic Oscillations*. 2024. arXiv: [2404.03002 \[astro-ph.CO\]](https://arxiv.org/abs/2404.03002). URL: <https://arxiv.org/abs/2404.03002>.
- [4] Scott Dodelson. *Modern cosmology*. San Diego, CA: Academic Press, 2003. URL: <https://cds.cern.ch/record/1282338>.
- [5] Aleksander Dolgov, Vitali Halenka, and Igor Tkachev. “Power-law cosmology, SN Ia, and BAO”. In: *Journal of Cosmology and Astroparticle Physics* 2014.10 (Oct. 2014), p. 047. DOI: [10.1088/1475-7516/2014/10/047](https://doi.org/10.1088/1475-7516/2014/10/047). URL: <https://dx.doi.org/10.1088/1475-7516/2014/10/047>.
- [6] Daniel J. Eisenstein et al. “Detection of the Baryon Acoustic Peak in the Large-Scale Correlation Function of SDSS Luminous Red Galaxies”. In: 633.2 (Nov. 2005), pp. 560–574. DOI: [10.1086/466512](https://doi.org/10.1086/466512). arXiv: [astro-ph/0501171 \[astro-ph\]](https://arxiv.org/abs/astro-ph/0501171).
- [7] Edwin Hubble. “A Relation between Distance and Radial Velocity among Extra-Galactic Nebulae”. In: *Proceedings of the National Academy of Science* 15.3 (Mar. 1929), pp. 168–173. DOI: [10.1073/pnas.15.3.168](https://doi.org/10.1073/pnas.15.3.168).

- [8] Fulvio Melia. “Strong observational support for the $Rh=ct$ timeline in the early universe”. In: *Physics of the Dark Universe* 46 (2024), p. 101587. ISSN: 2212-6864. DOI: <https://doi.org/10.1016/j.dark.2024.101587>. URL: <https://www.sciencedirect.com/science/article/pii/S2212686424001699>.
- [9] H. Mo, F. van den Bosch, and S. White. *Galaxy Formation and Evolution*. Galaxy Formation and Evolution. Cambridge University Press, 2010. ISBN: 9780521857932. URL: <https://books.google.fr/books?id=Zj7fDU3Z4wsC>.
- [10] S. Perlmutter et al. “Measurements of Ω and Λ from 42 high redshift supernovae”. In: *Astrophys. J.* 517 (1999), pp. 565–586. DOI: [10.1086/307221](https://doi.org/10.1086/307221). arXiv: [astro-ph/9812133](https://arxiv.org/abs/astro-ph/9812133).
- [11] Planck Collaboration et al. “Planck 2018 results. VI. Cosmological parameters”. In: 641, A6 (Sept. 2020), A6. DOI: [10.1051/0004-6361/201833910](https://doi.org/10.1051/0004-6361/201833910). arXiv: [1807.06209 \[astro-ph.CO\]](https://arxiv.org/abs/1807.06209).
- [12] Adam G. Riess et al. “Observational evidence from supernovae for an accelerating universe and a cosmological constant”. In: *Astron. J.* 116 (1998), pp. 1009–1038. DOI: [10.1086/300499](https://doi.org/10.1086/300499). arXiv: [astro-ph/9805201](https://arxiv.org/abs/astro-ph/9805201).
- [13] Adam G. Riess et al. “A Comprehensive Measurement of the Local Value of the Hubble Constant with 1 km s^{−1} Mpc^{−1} Uncertainty from the Hubble Space Telescope and the SH0ES Team”. In: *The Astrophysical Journal Letters* 934.1 (July 2022), p. L7. DOI: [10.3847/2041-8213/ac5c5b](https://doi.org/10.3847/2041-8213/ac5c5b). URL: <https://dx.doi.org/10.3847/2041-8213/ac5c5b>.
- [14] Ariel G. Sánchez et al. “The clustering of galaxies in the SDSS-III Baryon Oscillation Spectroscopic Survey: cosmological implications of the full shape of the clustering wedges in the data release 10 and 11 galaxy samples”. In: *Monthly Notices of the Royal Astronomical Society* 440.3 (Apr. 2014), pp. 2692–2713. ISSN: 0035-8711. DOI: [10.1093/mnras/stu342](https://doi.org/10.1093/mnras/stu342). eprint: <https://academic.oup.com/mnras/article-pdf/440/3/2692/23991261/stu342.pdf>. URL: <https://doi.org/10.1093/mnras/stu342>.
- [15] Daniel L. Shafer. “Robust model comparison disfavors power law cosmology”. In: *Phys. Rev. D* 91 (10 May 2015), p. 103516. DOI: [10.1103/PhysRevD.91.103516](https://doi.org/10.1103/PhysRevD.91.103516). URL: <https://link.aps.org/doi/10.1103/PhysRevD.91.103516>.
- [16] Isaac Tutzus et al. “Power law cosmology model comparison with CMB scale information”. In: *Phys. Rev. D* 94 (10 Nov. 2016), p. 103511. DOI: [10.1103/PhysRevD.94.103511](https://doi.org/10.1103/PhysRevD.94.103511). URL: <https://link.aps.org/doi/10.1103/PhysRevD.94.103511>.
- [17] Min Wang et al. “Testing the cosmic distance duality relation with Type Ia supernova and transverse BAO measurements”. In: *The European Physical Journal C* (July 2024). DOI: [10.1140/epjc/s10052-024-13049-1](https://doi.org/10.1140/epjc/s10052-024-13049-1).